Organometallics **2006,** *25,* 5165−5172 5165

Synthesis, Structural Characterization, and Reactivity of Lanthanide Complexes Containing a New Methylene-Bridged Indenyl−Pyrrolyl Dianionic Ligand

Chengfu Pi,[†] Zhengxing Zhang,[†] Ruiting Liu,[†] Linhong Weng,[†] Zhenxia Chen,[†] and Xigeng Zhou*[,†,‡]

Department of Chemistry, Shanghai Key Laboratory of Molecular Catalysis and Innovative Material, Fudan University, Shanghai 200433, People's Republic of China, and State Key Laboratory of Organometallic Chemistry, Shanghai 200032, People's Republic of China

Received July 6, 2006

A new methylene-bridged ligand incorporating both indenyl and pyrrolyl moieties, $(C_9H_7)CH_2(\alpha\text{-}C_4H_3\text{-}NH)$ (**1**), was prepared. Reaction of LnI_2 with 1 equiv of $[(C_9H_6)CH_2(\alpha\text{-}C_4H_3N)]Li_2(THF)_x$ in THF, followed by recrystallization in DME, gave the organolanthanide(II) complexes $\{(\eta^5\text{-}C_9H_6)CH_2[\mu\text{-}\eta^1\text{:}\eta^5\text{-}(\alpha\text{-}C_4H_3N)]Ln(DME)\}_2$ (Ln = Sm (**2**), Yb (**3**)) in mederate yields. Treatment of $SmCl_3$ with 1 equiv of $[(C_9H_6)CH_2(\alpha\text{-}C_4H_3N)]Li_2(THF)_x$ in THF gave the trivalent organosamarium chloride $\{(\eta^5\text{-}C_9H_6)CH_2\text{-}[\mu\text{-}\eta^1\text{:}\eta^5\text{-}(\alpha\text{-}C_4H_3N)]Sm(\mu\text{-}Cl)_2Li(THF)_2\}_2$ (**4**) in 73% yield, while reaction of $ErCl_3$ with $[(C_9H_6)CH_2\text{-}(\alpha\text{-}C_4H_3N)]Li_2(THF)_x$ under the same conditions generated $[(\eta^5\text{-}C_9H_6)CH_2(\mu\text{-}\eta^1\text{:}\eta^3\text{-}C_4H_3N)Er(\mu_3\text{-}Cl)(\mu\text{-}Cl)Li(THF)_2]_2$ (**5**). Reaction of **4** with 2 equiv of *n*-butyllithium (^{n}BuLi) and subsequently with *N*,*N*′-dicyclohexylcarbodiimide (CyN=C=NCy) gave the carbodiimide insertion into the Sm−C bond product $\{(\eta^5\text{-}C_9H_6)CH_2[\mu\text{-}\eta^1\text{:}\eta^5\text{-}(\alpha\text{-}C_4H_3N)]Sm[CyNC(^n\text{Bu})NCy]\}_2$ (**6**), while treatment of **4** with 2 equiv of $NaN(SiMe_3)_2$ in THF followed by reacting with CyN=C=NCy gave the carbodiimide insertion into the Sm−N bond product $[(\eta^5\text{-}C_9H_7)CH_2[\mu\text{-}\eta^1\text{:}\eta^5\text{-}(\alpha\text{-}C_4H_3N)]Sm\{CyNC[N(SiMe_3)_2]NCy\}]_2$ (**7**). These complexes were characterized by IR and ^{1}H NMR spectra and elemental analyses. Furthermore, the structures of all these compounds were also confirmed by X-ray diffraction analyses.

Introduction

The development of new ancillary ligands to support stoichiometric and catalytic reactivity at metal centers is currently an intensively studied area in organolanthanide chemistry.[1] Among strategies for the design of new ligands, *ansa* carbonous-bridged cyclopentadienyl ligands have received wide attention due to the often dramatic effects of the incorporation of the *ansa*-bridge on both the stability and the behavior of reactivity and catalytic activity of lanthanocene complexes.[2] Furthermore, the examination of alternatives to the commonly used cyclopentadienyl groups is also receiving special attention.[3] For example, it has been found that the *ansa*-dipyrrolyl ligand system has a promising feature with the formation of macrocyclic lanthanide clusters able to carry out four-electron reduction of dinitrogen.[4] In addition, the bimodal σ/π-bonding capability of this ligand provides the potential of retaining alkali cations, which proved to allow for the fine-tuning of the bonding model of the lanthanide center.[5] Despite the great development of various bridged cyclopentadienyl ligands and the emerging importance of the replacement of cyclopentadienyl groups with heterocyclic analogues, few studies have been reported on organolanthanide complexes containing the bridged hybrid cyclopentadienyl/heterocycle dianionic ligands.[1c]

To our knowledge, no example of bridged indenyl/pyrrolyl complexes has been reported to date. Given the rich chemistry of *ansa*-lanthanocene and/or *ansa*-dipyrrolyl lanthanide complexes and the greater reactivities of indenyl metal complexes compared to their cyclopentadienyl analogues,[6] we are interested to find out whether *ansa*-bridged indenyl−pyrrolyl complexes of lanthanides display the same variety of reactivities. We report here the synthesis and characterization of a series of organo-

---

* Corresponding author. E-mail: xgzhou@fudan.edu.cn.

[†] Shanghai Key Laboratory of Molecular Catalysis and Innovative Material.

[‡] State Key Laboratory of Organometallic Chemistry.

(1) (a) Schumann, H.; Meese-Marktscheffel, J. A.; Esser, L. *Chem. Rev.* **1995**, *95*, 865. (b) Arndt, S.; Okuda, J. *Chem. Rev.* **2002**, *102*, 1953. (c) Xie, Z. W. *Acc. Chem. Rev.* **2003**, *3*, 1. (d) Togni, A.; Halterman, R. L. *Metallocenes: Synthesis, Reactivity, Applications*; Wiley-VCH: New York, 1998; Vols. 1 and 2. (e) Arnold, P. L.; Liddle, S. T. *Organometallics* **2006**, *25*, 1485. (f) Patel, D.; Liddle, S. T.; Mungur, S. A.; Rodden, M.; Blake, A. J.; Arnold, P. L. *Chem. Commun.* **2006**, 1124. (g) Arnold, P. L.; Liddle, S. *Chem. Commun.* **2005**, 5638. (h) Liddle, S.; Arnold, P. L. *Organometallics* **2005**, *24*, 2597. (i) Cantat, T.; Jaroschik, F.; Ricard, L.; Le Floch, P.; Nief, F.; Mezailles, N. *Organometallics* **2006**, *25*, 1329. (j) Turcitu, D.; Nief, F.; Ricard, L. *Chem. Eur. J.* **2003**, *9*, 4916. (k) Cui, C.; Shafir, A.; Reeder, C. L.; Arnold, J. *Organometallics* **2003**, *22*, 3357.

(2) (a) Qian, C. T.; Nie, W. L.; Sun, J. *J. Organomet. Chem.* **2001**, *626*, 171. (b) Qian, C. T.; Nie, W. L.; Chen, Y. F.; Sun, J. *J. Organomet. Chem.* **2002**, *645*, 82. (c) Nie, W. L.; Qian, C. T.; Chen, Y. F.; Sun, J. *J. Organomet. Chem.* **2002**, *647*, 114.

(3) (a) Edelmann, F. T.; Freckmann, D. M. M.; Schumann, H. *Chem. Rev.* **2002**, *102*, 1851. (b) Dube, T.; Conoci, T.; Gambarotta, S.; Yap, G. P. A.; Vasapollo, G. *Angew. Chem., Int. Ed.* **1999**, *38*, 3657.

(4) (a) Dube, T.; Conoci, T.; Gambarotta, S.; Yap, G. P. A.; Vasapollo, G. *Angew. Chem., Int. Ed.* **1999**, *38*, 3657. (b) Dube, T.; Ganesan, M.; Conoci, S.; Gambarotta, S.; Yap, G. P. A *Organometallics* **2000**, *19*, 3716. (c) Dube, T.; Gambarotta, S.; Yap, G. P. A. *Organometallics* **2000**, *19*, 115. (d) Dube, T.; Conoci, S.; Gambarotta, S.; Yap, G. P. A. *Organometallics* **2000**, *19*, 1182. (e) Mani, G.; Lalonde, M. P.; Gambarotta, S.; Yap, G. P. A. *Organometallics* **2001**, *20*, 2443. (f) Ganesan, M.; Gambarotta, S.; Yap, G. P. A. *Angew. Chem., Int. Ed.* **2001**, *40*, 766. (g) Berube C. D.; Yazdanbakhsh, M.; Gambarotta, S.; Yap, G. P. A. *Organometallics* **2003**, *22*, 3742.

(5) (a) Ganesan, M.; Bérubé, C. D.; Gambarotta, S.; Yap, G. P. A. *Organometallics* **2002**, *21*, 1707.

(6) (a) Qian, C. T.; Zou, G.; Jiang, W. H.; Chen, Y. F.; Sun, J.; Li, N. *Organometallics* **2004**, *23*, 4980. (b) Qian, C. T.; Zou, G.; Chen, Y. F.; Sun, J. *Organometallics* **2001**, *20*, 3106.

10.1021/om060610t CCC: $33.50

lanthanide(II) and organolanthanide(III) complexes containing a new asymmetrically methylene-bridged indenyl and pyrrolyl ligand. The reactivities of their trivalent alkyl and amide derivatives toward *N*,*N*′-dicyclohexylcarbodiimide are also described.

Experimental Section

General Procedures. Except where noted, all manipulations were conducted in the absence of oxygen and water under an atmosphere of dinitrogen, either by use of standard Schlenk methods or within an mBraun glovebox apparatus. All organic solvents (including deuterated solvents for the NMR measurements) were dried and distilled under dinitrogen prior to use. Anhydrous $LnCl_3$ [7] and $LnI_2(THF)_x$ (Ln = Sm, Yb)[8] were prepared according to literature methods. All other chemicals were purchased from Aldrich Chemical Co. and used as received unless otherwise noted. Melting points were determined in sealed nitrogen-filled capillaries without temperature correction. Elemental analyses for C, H, and N were carried out on a Rapid CHN-O analyzer. Infrared spectra were obtained on a Nicolet FT-IR 360 spectrometer with samples prepared as Nujol mulls. ^1H NMR data were obtained on a Bruker DMX-500 NMR spectrometer.

Preparation of $(C_9H_7)CH_2(\alpha\text{-}C_4H_3NH)$ (1). To a CH_3OH solution (50 mL) of pyrrole-2-carboxaldehyde (5.1 g, 53.5 mmol) and indene (12.4 g, 107 mmol) was added pyrrolidine (7.6 g, 107 mmol) at rt. After stirring for 12 h, glacial AcOH (6.4 g, 107 mmol) was added to the dark red solution at 0 °C. The reaction mixture was diluted with ether (50 mL) and water (50 mL). The aqueous portion was extracted with Et_2O (50 mL × 4), and the combined organic portion was washed with water and brine and dried over anhydrous $MgSO_4$. Removal of solvent gave a pale yellow solid of fulvene-type indene compounds (5.0 g, 26.2 mmol, 49%), which was then added to a suspension of lithium aluminum hydride (0.89 g, 26.2 mmol) in THF (200 mL) in several portions at 0 °C. After stirring for 20 h, the mixture was quenched with water, then 10% HCl, extracted with diethyl ether (50 mL × 4), dried ($MgSO_4$), filtered, and concentrated. Reduced pressure distillation of the residues afforded **1** as a light yellow liquid, which solidified in a few days in a refrigerater. Yield: 2.82 g, 27% (based on pyrrole-2-carboxaldehyde). Mp: 27−28 °C. Anal. Calcd for $C_{14}H_{13}N$: C, 86.12; H, 6.71; N, 7.17. Found: C, 85.98; H, 6.68; N, 7.11. ^1H NMR (500 MHz, $CDCl_3$, 25 °C): δ 7.95 (br s, NH), 6.65 (d, 1H, C_4H_3NH), 6.16 (m, 1H, C_4H_3NH), 6.07 (s, 1H, C_4H_3NH), 3.93 (s, 2H, $-CH_2-$), 3.37 (s, CH_2, C_9H_7), 6.27 (s, 1H, C_9H_7), 7.46 (d, 1H, C_9H_7), 7.20−7.30 (m, 3H, C_9H_7). IR (Nujol, cm^{-1}): 3483 (w), 3415 (m), 1605 (m), 1560 (m), 1421(w), 1279 (w), 1261 (m), 1228 (m), 1195 (w), 1158 (w), 1113 (w), 1086 (m), 1028 (m), 962 (m), 914 (m), 880 (m), 799 (m), 775 (s), 721 (s), 648 (w).

Preparation of $\{(\eta^5\text{-}C_9H_6)CH_2[\mu\text{-}\eta^1{:}\eta^5\text{-}(\alpha\text{-}C_4H_3N)]Sm(DME)\}_2$ (2). To a THF solution of **1** (0.244 g, 1.25 mmol) (40 mL) held at 0 °C was dropwise added *n*-butyllithium (1.60 M in hexane, 1.56 mL, 2.50 mmol). The reaction mixture was stirred for 5 h at ambient temperature and turned slowly to orange. Then, a THF solution of SmI_2 (0.04 M, 31.3 mL, 1.25 mmol) was added at −30 °C. The reaction mixture was allowed to warm to room temperature. After stirring overnight, all volatiles were removed in vacuo to give a black, oily product, which was washed with hot toluene (5 mL × 3). The residue was extracted with DME (30 mL), and the solution was concentrated to ca. 10 mL and left at −15 °C for 3 days. **2** (0.27 g) was obtained as black crystals. Yield: 50%. Once crystallized, the complex is nearly insoluble in DME. Mp: 140−142 °C (dec). Anal. Calcd for $C_{36}H_{42}N_2O_4Sm_2$: C, 49.85; H, 4.88; N, 3.23; Sm, 34.67. Found: C, 49.67; H, 4.72; N, 3.09; Sm, 34.51. IR (Nujol, cm^{-1}): 3053 (m), 3037 (m), 2995 (m), 2720 (w), 1303 (w), 1209 (w), 1194 (w), 1148 (w), 1117 (w), 1071 (m), 1030 (m), 995 (w), 914 (w), 856 (m), 816 (w), 769 (w), 753 (w), 738 (w), 718 (m).

Preparation of $\{(\eta^5\text{-}C_9H_6)CH_2[\mu\text{-}\eta^1{:}\eta^5\text{-}(\alpha\text{-}C_4H_3N)]Yb(DME)\}_2$ (3). Following the procedure described for **2**, YbI_2 (0.04 M THF solution, 31.3 mL, 1.25 mmol) reacted with 1 equiv of dilithium salt of **1** to gave **3** as dark red blocks, yield: 0.24 g (42%). Mp: 128−130 °C (dec). Anal. Calcd for $C_{36}H_{42}N_2O_4Yb_2$: C, 47.37; H, 4.64; N, 3.07; Yb, 37.91. Found: C, 47.25; H, 4.43; N, 2.92; Yb, 37.70. ^1H NMR (pyridine-d_5): δ 9.01 (m, 14H), 7.77 (s, 4H), 5.50 (s, 4H), 4.93 (s, 4H), 4.71 (s, 12H), 3.64 (s, 4H). IR (Nujol, cm^{-1}): 3177 (m), 3078 (w), 2714 (w), 1329 (m), 1184 (m), 1146 (w), 1114 (m), 1069 (s), 1028 (m), 991 (w), 948 (m), 867 (s), 755 (m), 739 (s), 704 (w).

Preparation of $\{(\eta^5\text{-}C_9H_6)CH_2[\mu\text{-}\eta^1{:}\eta^5\text{-}(\alpha\text{-}C_4H_3N)]Sm(\mu\text{-}Cl)_2Li(THF)_2\}_2$ (4). To a THF (30 mL) solution of **1** (0.390 g, 2.00 mmol) held at 0 °C was added dropwise *n*-butyllithium in hexane (1.6 M, 2.5 mL, 4.00 mmol). After stirring at room temperature for 2 h, the resulting orange solution was added slowly to a suspension of $SmCl_3$ (0.513 g, 2.00 mmol) in THF (45 mL) with stirring at −78 °C. Then, the mixture was allowed to warm to room temperature and stirred for 24 h. The solution changed from colorless to light red during the course of the reaction. The solvent was evaporated under vacuum, leaving an oily residue that was washed with hexane (10 mL × 2). The resulting solid was extracted with THF (15 mL × 2). The solutions were combined and concentrated to about 10 mL, from which **4** was obtained as red-orange crystals after this solution stood at room temperature for 2 weeks (0.83 g, 73%). Mp: 121−123 °C (dec). Anal. Calcd for $C_{44}H_{54}Cl_4Li_2N_2O_4Sm_2$: C, 46.71; H, 4.81; N, 2.48. Found: C, 46.47; H, 4.63; N, 2.26. ^1H NMR (500 MHz, THF-d_8): δ 9.72 (br s, 2H, C_9H_7), 7.39 (d, 2H, C_9H_7), 7.30 (d, 2H, C_9H_7), 7.16(s, 2H, C_9H_7), 7.11(d, 2H, C_9H_7), 6.15 (d, 2H, C_9H_7), 6.54 (s, 2H, C_4H_3N), 5.93 (s, 2H, C_4H_3N), 5.87 (s, 2H, C_4H_3N), 3.29 (s, 4H, $-CH_2-$), 3.58 (br s, 16H, THF), 1.73 (br s, 16H, THF). IR (Nujol, cm^{-1}): 3120 (m), 3070 (m), 2900 (m), 1336 (m), 1039 (m), 958 (w), 859 (m), 769 (m), 723 (s).

Preparation of $[(\eta^5\text{-}C_9H_6)CH_2[\mu\text{-}\eta^1{:}\eta^3\text{-}(\alpha\text{-}C_4H_3N)]Er(\mu_3-Cl)(\mu\text{-}Cl)Li(THF)_2]_2$ (5). To a THF (30 mL) solution of **1** (0.390 g, 2.00 mmol) held at 0 °C was added dropwise *n*-butyllithium in hexane (1.6 M, 2.50 mL, 4.00 mmol). The reaction mixture was stirred at room temperature for 2 h. The resulting orange solution was added slowly to a suspension of $ErCl_3$ (0.547 g, 2.00 mmol) in THF (40 mL) with stirring at −78 °C, and the mixture was stirred for 24 h at room temperature. The solution changed from colorless to dark red. The solvent was evaporated under vacuum, leaving an oily residue, which was washed with hexane (10 mL × 2). The resulting solid was extracted with benzene (20 mL × 2). The solutions were combined and concentrated to about 20 mL. After standing at room temperature for several days, **5**$\cdot C_6H_6$ was obtained as pink crystals (0.696 g, 56%). Once crystallized, the complex is nearly insoluble in benzene. Mp: 131−133 °C (dec). Anal. Calcd for $C_{50}H_{60}Cl_4Er_2Li_2N_2O_4$: C, 48.30; H, 4.86; N, 2.25. Found: C, 48.08; H, 4.63; N, 2.11. IR (Nujol, cm^{-1}): 3057 (w), 3035 (m), 2900 (m), 1930 (w), 1604 (m), 1494 (w), 1401 (w), 1348 (w), 1338 (w), 1226 (m), 1166 (m), 1150 (w), 1136 (w), 1094 (m), 1031 (s), 959 (s), 913 (w), 866 (m), 802 (s), 762 (m), 739 (w), 729 (w), 695 (m), 661 (w), 622 (w).

Preparation of $\{(\eta^5\text{-}C_9H_6)CH_2[\mu\text{-}\eta^1{:}\eta^5\text{-}(\alpha\text{-}C_4H_3N)]Sm[CyNC(^nBu)NCy]\}_2$ (6). To a solution of **4** (1.13 g, 1.00 mmol) in THF (30 mL) was added *n*-butyllithium (1.6 M in *n*-hexane, 1.25 mL) at −30 °C. After stirring for 4 h, to the mixture was added *N*,*N*′-dicyclohexylcarbodiimide (0.412 g, 2.00 mmol) at −10 °C. The reaction mixture was then warmed to ambient temperature and stirred overnight. The solvent was removed by reduced pressure. The solid was extracted with benzene. The resulting yellow solution

---

[7] Taylor, M. D.; Carter, C. P. *J. Inorg. Nucl. Chem.* **1962**, *24*, 387

[8] Girard, P.; Namy, J. L.; Kagan, H. B. *J. Am. Chem. Soc.* **1980**, *102*, 2693.

Table 1. Crystal and Data Collection Parameters of Complexes 1, 2, 3, and 4

	1	2	3	4
formula	$C_{14}H_{13}N$	$C_{36}H_{42}N_2O_4Sm_2$	$C_{36}H_{42}N_2O_4Yb_2$	$C_{44}H_{54}Cl_4Li_2N_2O_4Sm_2$
molecular weight	195.25	867.42	912.80	1131.27
cryst color	colorless	black	black-red	red-yellow
cryst dimens (mm)	0.25 × 0.25 × 0.20	0.20 × 0.10 × 0.10	0.30 × 0.05 × 0.05	0.05 × 0.02 × 0.02
cryst syst	monoclinic	orthorhombic	orthorhombic	triclinic
space group	$P2_1/n$	$P2_12_12$	$P2_12_12$	$P\bar{1}$
unit cell dimens				
a (Å)	9.144(8)	13.719(5)	13.822(5)	10.200(7)
b (Å)	11.761(10)	18.172(6)	18.293(6)	10.495(7)
c (Å)	10.372(9)	8.247(3)	7.949(3)	11.609(8)
β (deg)	103.654(13)	90	90	93.357(11)
V (Å^3)	1084.0(16)	2056.1(12)	2010.0(12)	1175.0(13)
Z	4	2	2	1
D_c (g cm^{-3})	1.196	1.401	1.508	1.599
μ (mm^{-1})	0.070	2.861	4.658	2.743
F(000)	416	856	888	562
radiation (λ = 0.710730 Å)	Mo Kα	Mo Kα	Mo Kα	Mo Kα
temperature (K)	293.2	293.2	293.2	293.2
scan type	$\omega-2\theta$	$\omega-2\theta$	$\omega-2\theta$	$\omega-2\theta$
θ range (deg)	2.66 to 25.00	1.86 to 25.00	1.85 to 25.01	1.86 to 25.01
h,k,l range	$-10 \le h \le 5$, $-13 \le k \le 13$ $-12 \le l \le 12$	$-16 \le h \le 15$ $-21 \le k \le 20$ $-9 \le l \le 6$	$-16 \le h \le 13$ $-20 \le k \le 21$ $-9 \le l \le 9$	$-12 \le h \le 12$ $-12 \le k \le 12$ $-13 \le l \le 13$
no. of reflns measd	4412	7090	8408	5727
no. of unique reflns	1907 [R_{int} = 0.0340]	3567 [R_{int} = 0.0220]	3529 [R_{int} = 0.0417]	5727 [R_{int} = 0.0000]
completeness to θ	99.8% [θ = 25.00]	98.4% [θ = 25.01]	99.7% [θ = 25.01]	97.2% [θ = 25.01]
max. and min. transmn	0.9862 and 0.9828	0.7629 and 0.5985	0.8005 and 0.3355	0.9472 and 0.8751
refinement method	full-matrix least-squares on F^2			
no. of data/restraints/params	1907/0/136	3567/0/169	3529/0/199	5727/18/267
goodness-of-fit on F^2	1.029	1.065	1.066	0.946
final R indices [$I > 2\sigma(I)$]	R_1 = 0.0473, wR_2 = 0.1202	R_1 = 0.0514, wR_2 = 0.1565	R_1 = 0.0516, wR_2 = 0.1347	R_1 = 0.0906, wR_2 = 0.1828
R indices (all data)	R_1 = 0.0751, wR_2 = 0.1352	R_1 = 0.0694, wR_2 = 0.1733	R_1 = 0.0727, wR_2 = 0.1458	R_1 = 0.1307, wR_2 = 0.2056
largest diff peak and hole (e·Å^{-3})	0.210 and −0.151	1.548 and −0.531	1.460 and −0.599	3.804 and −2.718

was concentrated by reduced pressure to about 5 mL, and a yellow solid precipitated. The precipitate was resolved by addition of 2 mL of THF. Yellow crystals of **6**·C_6H_6 (0.96 g, 74%) were obtained upon standing at room temperature for a few days. Mp: 146−148 °C (dec). Anal. Calcd for $C_{68}H_{90}N_6Sm_2$: C, 63.20; H, 7.02; N, 6.50. Found: C, 63.01; H, 6.84; N, 6.32. ^{1}H NMR (500 MHz, benzene-d_6): 6.29 (s, 2H, C_4H_3N), 6.22 (s, 2H, C_9H_7), 6.09 (s, 2H, C_4H_3N), 5.88 (s, 2H, C_4H_3N), 3.03 (s, 4H, CH_2Ind), many broad, unresolved resonances. IR (Nujol, cm^{-1}): 3110 (w), 3065 (m), 3012 (m), 1649 (m), 1419 (w), 1361 (w), 1335 (w), 1276 (w), 1189 (m), 1175 (m), 1158 (m), 1088 (w), 1069 (w), 1039 (m), 1027 (m), 952 (s), 886 (m), 850 (m), 778 (m), 751 (s), 729 (s), 696 (s), 645 (v).

Preparation of [(η^5-C_9H_7)CH_2[μ-η^1:η^5-(α-C_4H_3N)]Sm{CyNC-[N(SiMe$_3$)$_2$]NCy}]$_2$ (7). To a solution of **4** (1.13 g, 1.00 mmol) in 30 mL of THF was added NaN(SiMe$_3$)$_2$ (0.267 g, 2.00 mmol) at 0 °C. After stirring at this temperature for 2 h, the mixture was warmed to room temperature and continued to stir for 5 h. The precipitate (NaCl) was removed by centrifugation. Then, to the clear solution was added *N*,*N*′-dicyclohexylcarbodiimide (0.412 g, 2.00 mmol) at −30 °C. After stirring for 2 h at −30 °C, the mixture was slowly warmed to ambient temperature and was further stirred for 24 h. Removal of the solvent left a pale yellow solid. The resulting solid was extracted with 60 mL of benzene, followed by filtration. The extract was evaporated to ca. 20 mL. Red-yellow crystals of **7**·4THF·C_6H_6 were slowly formed at room temperature. Yield: 1.09 g (61%). Mp: 106−108 °C. Anal. Calcd for $C_{88}H_{140}N_8O_4Si_4Sm_2$: C, 59.14; H, 7.90; N, 6.27. Found: C, 58.95; H, 7.72; N, 6.13. ^{1}H NMR (500 MHz, benzene-d_6): 3.55 (s, 16H, free THF), 3.04 (s, 4H, CH_2Ind), 1.80, 1.60 (2 brm, together, 22H, C_6H_{11}), 1.45 (s, 16H, free THF), 1.24 (m, 22H, C_6H_{11}), 0.27, 0.22 (2 s, 36H, SiMe$_3$), plus many broad, unresolved peaks. IR (Nujol, cm^{-1}): 3080 (w), 3046 (m), 2950 (w), 1629 (m), 1342 (w), 1291 (w), 1173 (m), 1071 (m), 994 (m), 953 (m), 938 (m), 777 (m), 750 (m), 722 (m).

X-ray Structural Determination. Suitable single crystals were sealed under N_2 in thin-walled glass capillaries. Data were collected at 293.2 K on a Bruker SMART Apex CCD diffractometer using graphite-monochromated Mo Kα (λ = 0.71073 Å) radiation. During the intensity data collection, no significant decay was observed. The intensities were corrected for Lorentz−polarization effects and empirical absorption with the SADABS program.[9] The structures were solved by direct methods using the SHELXL-97 program.[10] All non-hydrogen atoms were found from the difference Fourier syntheses. The H atoms were included in calculated positions with isotropic thermal parameters related to those of the supporting carbon atoms but were not included in the refinement. All calculations were performed using the Bruker Smart program. The absolute configuration of **2** was assigned by anomalous dispersion effects in diffraction measurements on the crystal, while the absolute structure of **3** has not been established by anomalous dispersion effects in diffraction measurements on the crystal, for which an arbitrary choice of enantiomer has been made. Crystal data and details of data collection and structure refinements are given in Tables 1 and 2, respectively. Selected bond distances and angles are compiled in Tables 3−8, respectively. Further details are included in the Supporting Information.

Results and Discussion

Synthesis of Indenylpyrrolylmethane. [(C_9H_7)CH_2(α-C_4H_3-NH)] (**1**) was readily prepared by the reaction of pyrrole-2-

---

[9] Sheldrick, G. M. *SADABS*, A Program for Empirical Absorption Correction; University of Göttingen: Göttingen, Germany, 1998.

Table 2. Crystal and Data Collection Parameters of Complexes 5, 6, and 7

	5·C_6H_6	**6**·C_6H_6	**7**·4THF·C_6H_6
formula	$C_{50}H_{60}Cl_4Er_2Li_2N_2O_4$	$C_{68}H_{90}N_6Sm_2$	$C_{88}H_{140}N_8O_4Si_4Sm_2$
molecular weight	1243.20	1292.16	1787.14
cryst color	pale orange	yellow	red-yellow
cryst dimens (mm)	0.15 × 0.10 × 0.10	0.10 × 0.08 × 0.05	0.20 × 0.10 × 0.10
cryst syst	monoclinic	triclinic	triclinic
space group	$P2_1/c$	$P\bar{1}$	$P\bar{1}$
unit cell dimens			
a (Å)	11.699(4)	9.215(2)	11.566(4)
b (Å)	18.752(6)	11.225(3)	13.722(5)
c (Å)	12.686(4)	15.391(4)	15.778(5)
β (deg)	110.629(4)	92.436(5)	105.602(4)
V (Å^3)	2604.5(14)	1563.5(7)	2281.1(13)
Z	2	1	1
D_c (g cm^{-3})	1.585	1.372	1.301
μ (mm^{-1})	3.448	1.903	1.378
F(000)	1232	664	936
radiation ($\lambda = 0.710730$Å)	Mo Kα	Mo Kα	Mo Kα
temperature (K)	293.2	293.2	293.2
scan type	$\omega-2\theta$	$\omega-2\theta$	$\omega-2\theta$
θ range (deg)	1.86 to 26.01	1.85 to 25.01	1.36 to 25.01
h,k,l range	$-14 \le h \le 10$	$-10 \le h \le 10$	$-13 \le h \le 13$,
	$-23 \le k \le 22$	$-12 \le k \le 13$	$-16 \le k \le 16$
	$-5 \le l \le 15$	$-18 \le l \le 16$	$-10 \le l \le 18$
no. of reflns measd	11 654	6627	9566
no. of unique reflns	5102 [$R_{int} = 0.0305$]	5441 [$R_{int} = 0.0631$]	7893 [$R_{int} = 0.0163$]
completeness to θ	99.6% [$\theta = 26.01$]	98.7% [$\theta = 25.01$]	98.3% [$\theta = 25.01$]
max. and min. transmn	0.7243 and 0.6258	0.9108 and 0.8325	0.8745 and 0.7702
refinement method	full-matrix least-squares on F^2		
no. of data/restraints/params	5102/10/289	5441/11/343	7893/31/418
goodness-of-fit on F^2	1.135	1.025	1.087
final R indices [$I > 2\sigma(I)$]	$R_1 = 0.0349$, $wR_2 = 0.0809$	$R_1 = 0.0742$, $wR_2 = 0.1427$	$R_1 = 0.0437$, $wR_2 = 0.1175$
R indices (all data)	$R_1 = 0.0621$, $wR_2 = 0.0976$	$R_1 = 0.1257$, $wR_2 = 0.1649$	$R_1 = 0.0611$, $wR_2 = 0.1348$
largest diff. peak and hole (e·Å^{-3})	1.189 and −0.666	1.801 and −0.782	1.000 and −0.711

Table 3. Selected Bond Lengths [Å] and Angles [deg] for Complex 1

N(1)−C(1)	1.365(3)	C(5)−C(6)	1.503(3)
N(1)−C(4)	1.366(3)	C(6)−C(7)	1.339(3)
C(1)−C(2)	1.342(3)	C(6)−C(10)	1.468(3)
C(2)−C(3)	1.408(3)	C(7)−C(8)	1.497(3)
C(3)−C(4)	1.356(3)	C(8)−C(9)	1.503(3)
C(4)−C(5)	1.495(3)	C(9)−C(10)	1.405(3)
N−H···centroid(benzene ring)	2.47		
C(4)−C(5)−C(6)	115.05(16)	C(7)−C(6)−C(5)	128.20(19)
C(3)−C(4)−C(5)	130.74(18)		

Table 4. Selected Bond Lengths [Å] and Angles [deg] for Complexes 2 and 3

	2	**3**		**2**	**3**
Ln	Sm	Yb	Ln	Sm	Yb
Ln1−N(1)	2.602(11)	2.456(12)	Ln1−C(8)	2.843(11)	2.686(14)
Ln1A−N(1A)	2.829(9)	2.790(11)	Ln1−C(9)	2.816(12)	2.734(14)
Ln1−O(1)	2.581(11)	2.490(11)	Ln1A−C(11A)	2.920(12)	2.875(14)
Ln1−O(2)	2.578(12)	2.460(11)	Ln1A−C(12A)	2.973(11)	2.865(15)
Ln1−C(1)	2.868(12)	2.861(17)	Ln1A−C(13A)	2.914(12)	2.796(15)
Ln1−C(6)	2.891(11)	2.841(13)	Ln1A−C(14A)	2.794(13)	2.743(14)
Ln1−C(7)	2.855(11)	2.743(14)	Ln1···Ln1A	4.281	4.166
N(1)−Ln−O(2)	86.2(3)	84.6(4)	N(1)−Ln1−N(1A)	72.7(4)	71.4(4)
N(1)−Ln1−O(1)	151.5(3)	149.7(4)	C(11)−C(10)−C(7)	114.6(11)	115.6(13)
O(2)−Ln1−O(1)	65.4(4)	65.1(4)	Ln1−N(1)−Ln1A	103.9(3)	104.9(4)
C(10)−C(7)−Ln1	113.3(8)	111.7(9)			

carboxaldehyde with indene catalyzed by pyrrolidine (Scheme 1). **1** is soluble in some common organic solvents. The formulation of **1** was confirmed through a single-crystal X-ray diffraction study. Figure 1 and Table 3 provide a summary of these results. No isomers in this solid were detected by ^{1}H NMR spectrometry.

In the solid state, compound **1** is present as pairs of enantiomeric molecules with a center of inversion. There is no intermolecular hydrogen bonding, and aggregation into dimers is based on parallel head-to-tail stacking with only weak centroid

---

(10) Sheldrick, G. M. *SHELXL-97*, Program for the Refinement of Crystal Structures; University of Göttingen: Göttingen, Germany, 1997.

Table 5. Selected Bond Lengths [Å] and Angles [deg] for Complex 4

Sm(1)−N(1)	2.468(13)	Cl(1)−Li(1)	2.36(4)
Sm(1)−N(1A)	2.824(12)	Cl(2)−Li(1)	2.25(4)
Sm(1)−C(4)	2.691(19)	N(1)−Sm(1A)	2.824(12)
Sm(1)−C(1)	2.72(2)	C(11)−Sm(1A)	2.829(18)
Sm(1)−C(3)	2.72(2)	C(12)−Sm(1A)	2.834(17)
Sm(1)−Cl(1)	2.730(6)	C(13)−Sm(1A)	2.715(15)
Sm(1)−C(5)	2.733(17)	C(14)−Sm(1A)	2.702(16)
Sm(1)−C(2)	2.746(19)	O(1)−Li(1)	2.02(4)
Sm(1)−Cl(2)	2.795(5)	O(2)−Li(1)	1.87(4)
Sm(1)···Sm(1A)	4.422		
N(1)−Sm(1)−Cl(1)	78.9(4)	O(2)−Li(1)−O(1)	106.3(18)
N(1)−Sm(1)−Cl(2)	157.1(3)	O(2)−Li(1)−Cl(2)	120(2)
Cl(1)−Sm(1)−Cl(2)	79.08(17)	O(1)−Li(1)−Cl(2)	113.5(18)
N(1)−Sm(1)−N(1A)	66.8(4)	O(2)−Li(1)−Cl(1)	106.5(18)
C(10)−C(4)−Sm(1)	111.9(13)	O(1)−Li(1)−Cl(1)	110.9(19)
C(11)−C(10)−C(4)	110.8(17)	Cl(2)−Li(1)−Cl(1)	99.2(14)
Sm(1)−N(1)−Sm(1A)	113.2(4)		

Table 6. Selected Bond Lengths [Å] and Angles [deg] for Complex 5

Er(1)−O(1)	2.346(4)	Er(1)−Cl(1)	2.814(2)
Er(1)−N(1)	2.367(5)	Cl(1)−Li(1)	2.715(19)
Er(1)−C(3)	2.627(6)	Cl(1)−Er(1A)	2.718(2)
Er(1)−C(1)	2.637(6)	Cl(2)−Li(1)	2.297(14)
Er(1)−C(2)	2.638(6)	Li(1)−N(1A)	2.153(14)
Er(1)−Cl(2)	2.657(16)	Li(1)−C(11A)	2.686(15)
Er(1)−C(5)	2.694(6)	Li(1)−C(14A)	2.448(16)
Er(1)−C(4)	2.695(6)	O(2)−Li(1)	1.908(15)
Er(1)−Cl(1A)	2.718(2)	O(2)−Li(1)−Cl(2)	112.0(6)
O(1)−Er(1)−N(1)	86.82(17)	O(2)−Li(1)−Cl(1)	108.2(8)
O(1)−Er(1)−Cl(2)	85.87(12)	O(2)−Li(1)−N(1A)	121.2(7)
N(1)−Er(1)−Cl(1A)	85.43(13)	O(2)−Li(1)−Cl(2)	112.0(6)
Cl(2)−Er(1)−Cl(1A)	93.10(5)	O(2)−Li(1)−C(14A)	131.6(9)
Cl(2)−Er(1)−Cl(1)	78.83(5)	O(2)−Li(1)−C(11A)	91.3(6)
Cl(1A)−Er(1)−Cl(1)	73.91(5)	O(2)−Li(1)−Cl(1)	108.2(8)
Li(1)−Cl(1)−Er(1)	87.2(3)	N(1A)−Li(1)−Cl(1)	89.8(6)
Er(1A)−Cl(1)−Er(1)	106.09(5)	Cl(2)−Li(1)−Cl(1)	87.4(5)
Li(1)−Cl(2)−Er(1)	100.5(4)	O(2)−Li(1)−Cl(2)	112.0(6)
C(11)−N(1)−Er(1)	122.1(4)		

Table 7. Selected Bond Lengths [Å] and Angles [deg] for Complex 6

Sm(1)−N(2)	2.391(9)	Sm(1)−C(20)	2.816(11)
Sm(1)−N(1)	2.438(9)	N(3)−Sm(1A)	2.592(8)
Sm(1)−N(3A)	2.592(8)	C(28)−Sm(1A)	2.844(10)
Sm(1)−C(26)	2.715(10)	C(29)−Sm(1A)	2.831(10)
Sm(1)−C(18)	2.734(10)	C(30)−Sm(1A)	2.796(11)
Sm(1)−C(19)	2.766(10)	C(31)−Sm(1A)	2.747(11)
Sm(1)−C(25)	2.779(10)	Sm(1)···Sm(1A)	4.507
Sm(1)−N(3)	2.809(9)		
N(2)−Sm(1)−N(1)	55.2(3)	N(1)−C(13)−C(14)	121.7(10)
N(2)−Sm(1)−N(3A)	96.1(3)	N(2)−C(13)−C(14)	122.3(10)
N(3A)−Sm(1)−C(26)	65.0(3)	Sm(1A)−N(3)−Sm(1)	113.1(3)
N(1)−C(13)−N(2)	116.1(10)	N(3A)−Sm(1)−N(3)	66.9(3)

Table 8. Selected Bond Lengths [Å] and Angles [deg] for Complex 7

Sm(1)−N(3)	2.432(4)	Sm(1)−C(7)	2.739(5)
Sm(1)−N(2)	2.444(4)	Sm(1)−C(8)	2.780(6)
Sm(1)−N(1)	2.566(4)	Sm(1)−C(10)	2.798(6)
Sm(1)−C(6)	2.698(5)	Sm(1)−N(1A)	2.840(4)
N(1)−Sm(1A)	2.840(4)	C(4)−Sm(1A)	2.836(6)
C(1)−Sm(1A)	2.815(5)	C(3)−Sm(1A)	2.840(6)
C(2)−Sm(1A)	2.817(6)	Sm(1)···Sm(1A)	4.570
N(2)−C(15)	1.307(7)	N(3)−C(22)	1.476(7)
N(2)−C(16)	1.472(7)	N(3)−C(22)	1.476(7)
N(3)−C(15)	1.346(7)	N(4)−C(15)	1.456(7)
N(1)−Sm(1)−N(1A)	64.6(2)	N(2)−C(15)−N(3)	114.5(5)
Sm(1)−N(1)−Sm(1A)	115.4(2)	N(2)−C(15)−N(4)	123.4(5)
N(1)−Sm(1)−C(6)	65.0(2)	N(3)−C(15)−N(4)	122.1(5)
N(3)−Sm(1)−N(1)	94.3(1)	N(3)−Sm(1)−N(2)	54.4(2)

Scheme 1

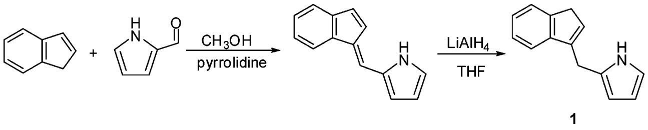

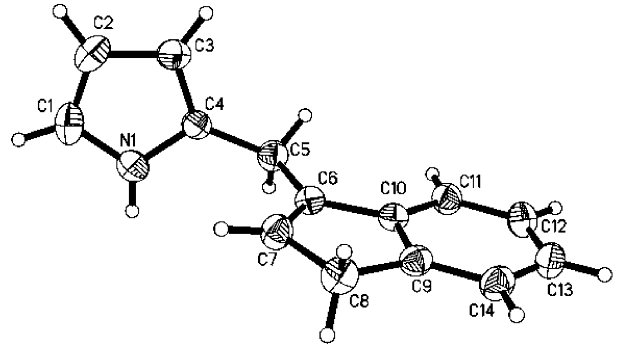

Figure 1. ORTEP diagram of **1** with the probability ellipsoids drawn at the 30% level.

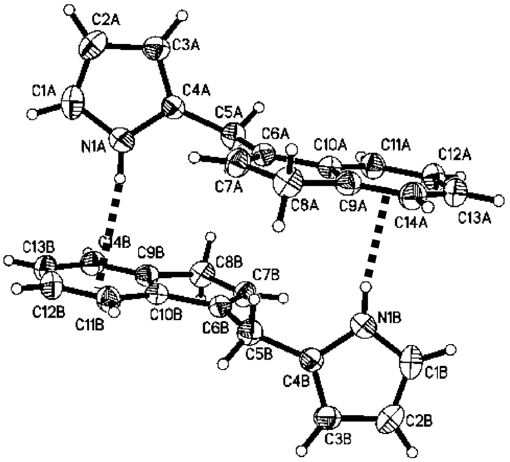

Figure 2. Pairs of enantiomeric molecules of **1** in the crystal (arbitrary radii). Hydrogen atoms on the N atom of the pyrrolyl in the ligand are in a "phenyl-embraced" orientation.

phenyl embrace interactions between N-H functions and benzene rings (Figure 2). The two components of these dimeric units show no $\pi-\pi$ stacking (the indene parts are not facing each other) but each has a H−N bond pointing toward a center of a benzene ring of a neighboring indene moiety. The H−centroid (benzene ring) distance is 2.47 Å and is shorter than the previously observed value of 2.79 Å.[11]

Synthesis and Characterization of *ansa*-Bridged Indenyl/Pyrrolyl Complexes of Lanthanides(II) $\{(\eta^5\text{-}C_9H_6)CH_2[\mu\text{-}\eta^1{:}\eta^5\text{-}(\alpha\text{-}C_4H_3N)]Ln(DME)\}_2$ (Ln = Sm, Yb). Treatment of $C_9H_7CH_2(\alpha\text{-}C_4H_3NH)$ with 2 equiv of *n*-butyllithium in THF followed by reacting with $LnI_2(THF)_x$ afforded the neutral complexes $\{(\eta^5\text{-}C_9H_6)CH_2[\mu\text{-}\eta^1{:}\eta^5\text{-}(\alpha\text{-}C_4H_3N)]Ln(DME)\}_2$ [Ln = Sm (**2**), Yb (**3**)] in mederate yields (Scheme 2). In sharp contrast to *ansa*-bridged dipyrrolides of divalent rare earths, which are precursors to dinitrogen reduction,[12] exposure of **2** and **3** to nitrogen gas or carrying out the above preparation

---

[11] Adams, H.; Harris, K. D. M.; Hembury, G. A.; Hunter, C. A.; Livingstone, D.; McCabe, J. F. *Chem. Commun.* **1996**, 2531.

[12] (a) Evans, W. J.; Rabe, G. W.; Ziller, J. W. *Organometallics* **1994**, *13*, 1641. (b) Edelmann, F. T. *Coord. Chem. Rev.* **1995**, *137*, 403. (c) Minhas, R.; Song, J.; Ma, Y.; Gambarotta, S. *Inorg. Chem.* **1996**, *35*, 1866. (d) Evans, J. W.; Ansari, M. A.; Ziller, J. W. *Inorg. Chem.* **1996**, *35*, 5435.

Scheme 2

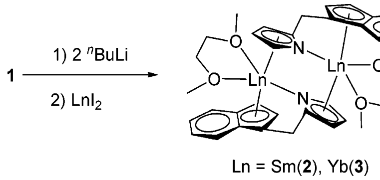

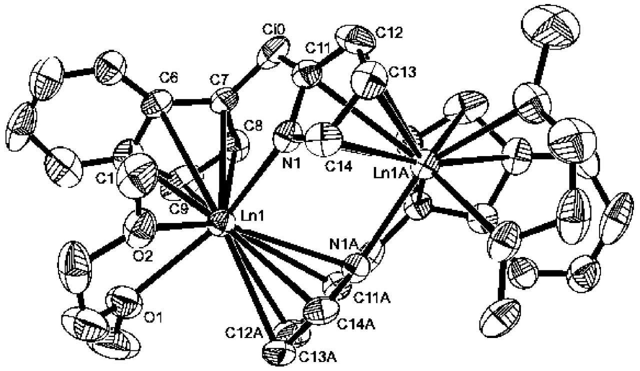

Figure 3. ORTEP diagram of **2** and **3** with the probability ellipsoids drawn at the 30% level. Hydrogen atoms are omitted for clarity.

directly under an N_2 atmosphere did not afford any dinitrogen complex but yielded instead intractable compounds. Complexes **2** and **3** are very air- and moisture-sensitive. **3** is readily dissolved in THF and DME, but **2** is sparing soluble in these solvents.

As shown in Figure 3, complexes **2** and **3** are isostructural, in which the *ansa*-bridged indenyl/pyrrolyl ligand acts as a tridentate dianion, with the pyrrolyl being both σ-bonded to one lanthanide ion and π-bonded to another metal, resulting in a symmetrical bimetallic structure. Each metal is η^1-bonded to two oxygen atoms of DME and one N atom of the pyrrolyl moiety and η^5-bonded to one indenyl group and the pyrrolyl group from another *ansa*-bridged indenyl/pyrrolyl ligand. The coordination geometry about each Ln^{2+} ion may be viewed as a distorted triangle bipyramid, in which one σ-bonded nitrogen atom and two donating O atoms of DME define the equatorial plane, while the centroid of the η^5-bonded cyclopentadienyl ring in the indenyl group and that of the η^5-bonded pyrrole ring of the adjacent ligand occupying the axial positions. Obviously, the bonding mode of the pyrrolyl ring in the present ligand is similar to those in the *ansa*-dipyrrolyl lanthanide complexes,[4] but is different from the observation in *ansa*-bridged cyclopentadienyl/pyrrolyl titanium complexes, where the pyrrolyl group is bound to metal only in a σ-mode through the nitrogen atom.[13] Combustion analysis data of **4** and **5** were in good agreement with the formulation as elucidated by the X-ray crystal structural analysis.

The indenyl group in **2** shows η^5-coordination to the samarium atom with normal distances ranging from 2.816(12) to 2.891(11) Å, and the average Sm−C(Ind) distance of 2.855(11) Å is similar to those found in *meso*-$O(CH_2CH_2C_9H_6)_2Sm(DME)$ (average 2.875 Å),[14] while in **3** the indenyl group exhibits a pronounced “slip-fold” distortion relative to a planar η^5-indenyl ligand, so that the Cp part of indenyl moiety tends to be an $\eta^3 + \eta^2$ type ligand and bent over the C7 and C9 axis by 10°; the distances of nodal carbon atoms C1 and C6 to the

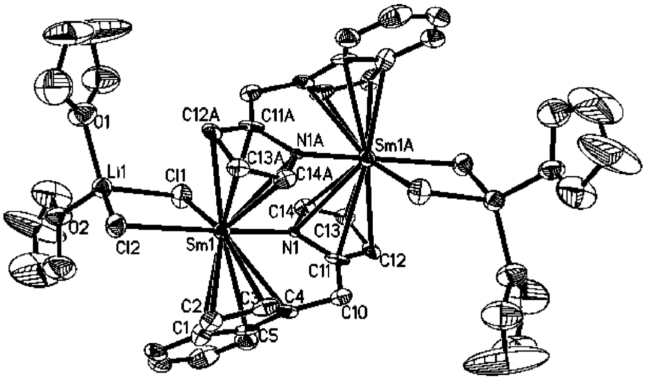

Figure 4. ORTEP diagram of **4** with the probability ellipsoids drawn at the 30% level. Hydrogen atoms are omitted for clarity.

Scheme 3

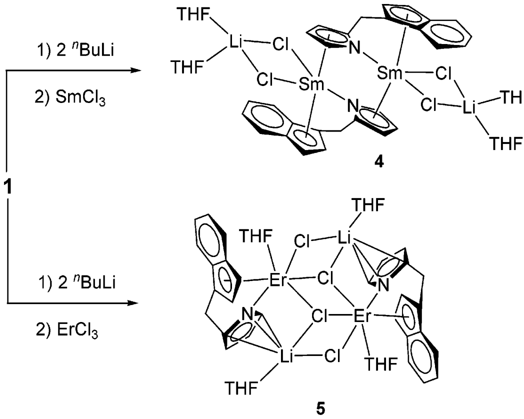

Yb^{2+} ion are 2.861(17) and 2.841(13) Å, respectively. The Yb−C bond distances of an allylic (C7, C8, and C9) fragment range from 2.686(14) to 2.743(14) Å, with the central carbon atom (C8) somewhat nearer to the metal than the terminal ones. These results show that the tendency to slip toward η^3- from η^5-mode for the indenyl group increases with “the contraction effect of lanthanides”. The average Sm−O(DME) distance of 2.58(1) Å in **2** is similar to the corresponding value in *meso*-$O(CH_2CH_2C_9H_6)_2Sm(DME)$, 2.576(5) Å.[14] The Sm1−N1 distance (2.602(11) Å) in **2** is similar to that found in $\{[Et_2C(\alpha\text{-}C_4H_3N)_2]Sm\}_8(THF)_4$, 2.617(10) Å.[4h] All bond parameters for **3** are in normal ranges (Table 4). The bond distances involving the metal in **3** are similar to the corresponding values in **2**, if the difference in metal radii is considered.[15]

Synthesis and Characterization of *ansa*-Bridged Indenyl/Pyrrolyl Lanthanide(III) Chloride Complexes. Reaction of $SmCl_3$ with 1 equiv of $(C_9H_6)CH_2(\alpha\text{-}C_4H_3N)Li_2(THF)_x$ in THF formed the dimeric organolanthanide complex $\{(\eta^5\text{-}C_9H_6)CH_2\text{-}[\mu\text{-}\eta^1\text{:}\eta^5\text{-}(\alpha\text{-}C_4H_3N)]Sm(\mu\text{-}Cl)_2Li(THF)_2\}_2$ (**4**) in 73% yield, while treatment of $ErCl_3$ with 1 equiv of $(C_9H_6)CH_2(\alpha\text{-}C_4H_3N)\text{-}Li_2(THF)_x$ under the same reaction conditions gave $\{(\eta^5\text{-}C_9H_6)\text{-}CH_2[\mu\text{-}\eta^1\text{:}\eta^3\text{-}(\alpha\text{-}C_4H_3N)]Er(\mu_3\text{-}Cl)(\mu\text{-}Cl)Li(THF)_2\}_2$ (**5**) in 56% yield (Scheme 3). They remain air- and moisture-sensitive, whether in the solid or solution phase. These complexes are readily dissolved in THF, but nearly insoluble in benzene, toluene, and hexane at room temperature. The molecular structures of **4** and **5** were confirmed by X-ray analyses, as shown in Figures 4 and 5. The paramagnetic erbium complex **5** does not offer useful NMR information. However, the paramagnetic samarium complex **4** provides interpretable NMR data.

---

(13) Seo, W. S.; Cho, Y. J.; Yoon, S. C.; Park, J. T.; Park, Y. *J. Organomet. Chem.* **2001**, *640*, 79.

(14) Qian, C. T.; Zou G.; Jiang, W. H.; Chen, Y. F.; Sun J.; Li, N. *Organometallics* **2004**, *23*, 4980.

(15) Shannon, R. D. *Acta Crystallogr. Sect. A* **1976**, *38*, 75.

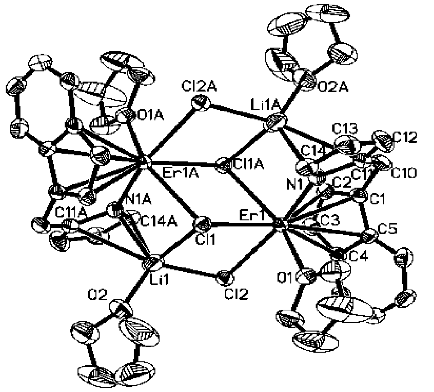

Figure 5. ORTEP diagram of **5** with the probability ellipsoids drawn at the 30% level. Hydrogen atoms are omitted for clarity.

In the solid, complex **4** is comprised of two samarium atoms ($Sm1\cdots Sm1A = 4.422$ Å) held together by two pyrrolyl rings of different ligands. Each Sm^{3+} ion is σ-bonded to two bridging Cl atoms and one N atom from the pyrrolyl ring and η^5-bonded to one five-membered ring of the indenyl group and one pyrrolyl ring of the adjacent *ansa*-ligand, which in turn is also both σ-bonded and π-bonded to the other Sm atom. The samarium atoms adopt a distorted trigonal-bipyramidal conformation with two chlorides and one nitrogen atom of the σ-bonded ring occupying the equatorial positions and one π-bonded pyrrolyl centroid and one π-bonded five-membered ring of the indenyl group occupying the axial positions. Two lithium atoms are also part of the structure. Each Li atom bonded to two THF molecules [$Li1-O1 = 2.02(4)$ Å; $Li1-O2 = 1.87(4)$ Å] is attached to two bridging chlorines to form a distorted-tetrahedral geometry.

Figure 5 shows the structure of **5**. In sharp contrast to **4**, the *ansa*-bridged indenyl/pyrrolyl ligand in **5** chelates the Er^{3+} ion with one nitrogen atom and one η^5-indenyl group and bridges one Li^+ ion in η^3-fashion, forming a tetrametallic cluster structure. Each Er^{3+} ion is η^5-bound to one five-membered ring of the indenyl group and σ-bound to one N atom of the pyrrolyl ring, one doubly bridging Cl atom, and two triply bridging Cl atoms and one O atom of THF in a distorted-octahedral arrangement. The structure also incorporates two lithium atoms, and each lithium atom is coordinated to η^3-pyrrolyl, one doubly bridging Cl atom, and one triply bridging Cl atom and one THF O atom in a distorted-tetrahedral arrangement.

Although Er^{3+} ions did not π-bond to the pyrrolyl ring, two lithium atoms are both π-bonded to the pyrrolyl ring and located toward the exterior of the molecule **5**, and one molecule of THF and two bridging Cl anions complete the coordination sphere of the each lithium atoms. These bond distances ($Li1-N1A$ 2.153(14) Å; $Li1-C14A$ 2.448(16) Å; $Li1-C11A$ 2.686(16) Å) are comparable with those in $[Ph_2C(\alpha\text{-}C_4H_3N)_2]_2Li_4(OEt_2)_3$.[16]

The structural difference between **4** and **5** gives new insight into the effect of the lanthanide contraction on the structure.[17] It is interesting to note that **5** adopts a eight-coordinated cluster structure as opposed to the nine-coordinated linear structure of **4**. Obviously, it is possible that the steric factor favors the observed cluster structure over a linear alternative, and the increased steric effect resulting from the lanthanide contraction would cause unfavorable contacts between the indenyl group and the pyrrolyl ring. Therefore the observed low coordination of erbium by pyrrolyl rings is accepted on account of favorable packing of the cluster.

Scheme 4

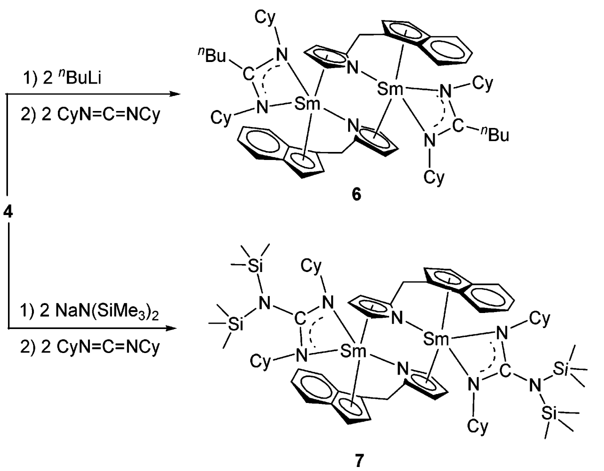

Reactivity of *ansa*-Bridged Indenyl/Pyrrolyl Lanthanide(III) Alkyl and Amido Complexes toward *N,N*-Dicyclohexylcarbodiimide. Recently, insertions of carbodiimides into the lanthanide−ligand bonds have attracted considerable attention.[18] Complexes **4** and **5** represent rare structurally characterized examples of organolanthanide compounds bearing both a Ln−pyrrolyl bond and a Ln−Cl bond, in which the chlorine atoms can be expected to be replaced by other groups via salt metathesis reactions.[4a,c,19,] To further study the effects of the nature of co-ligands on the carbodiimide insertion reaction and to examine whether the lanthanide−pyrrolyl bond was reactive to unsaturated substrates, we synthesized in situ the alkyl derivative $[(C_9H_6)CH_2(\alpha\text{-}C_4H_3N)]Sm(^nBu)(THF)_x$ by the treatment of **4** with 2 equiv of Li^nBu in THF and studied its reaction with *N,N′*-dicyclohexylcarbodiimide, as shown in Scheme 4.

Like the corresponding nonbridged lanthanocene alkyl species, $[(C_9H_6)CH_2(\alpha\text{-}C_4H_3N)]Sm(^nBu)(THF)_x$ also exhibits high reactivity toward unsaturated substrates. It reacts with 1 equiv of *N,N*-dicyclohexylcarbodiimide in THF at −10 °C to give the monoinsertion product (**6**). But attempts to further insert one carbodiimide into the Ln−N(pyrrolyl) bond were unsuccessful even when a large excess of *N,N′*-dicyclohexylcarbodiimide was added with a higher reaction temperature and a prolonged reaction time.

To obtain additional data on *ansa*-bridged indenyl/pyrrolyl lanthanide systems, we then turned to the reactivity of the amide derivative of **4**. The metathesis reaction of **4** with 2 equiv of $NaN(SiMe_3)_2$, followed by treating with *N,N′*-dicyclohexylcarbodiimide, allowed the isolation of the Ln−N bond insertion product $[(\eta^5\text{-}C_9H_7)CH_2[\mu\text{-}\eta^1{:}\eta^5\text{-}(\alpha\text{-}C_4H_3N)]Sm\{CyNC[N(SiMe_3)_2]\text{-}NCy\}]_2$ (**7**) in 61% yield (Scheme 4).

---

(16) Aharonian, G.; Gambarotta, S.; Yap, G. P. A. *Organometallics* **2002**, *21*, 4257.

(17) Study along this line is currently underway in our labs, and the results will be published later.

(18) (a) Zhang, J.; Ruan, R. Y.; Shao, Z. H.; Cai, R. F.; Weng, L. H.; Zhou, X. G. *Organometallics* **2002**, *21*, 1420. (b) Zhang, J.; Cai, R. F.; Weng, L. H.; Zhou, X. G. *J. Organomet. Chem.* **2003**, *672* (1−2), 94. (c) Zhang J.; Cai R. F.; Weng L. H.; Zhou X. G. *Organometallics* **2003**, *22*, 5385. (d) Zhang, J.; Cai, R. F.; Weng, L. H.; Zhou, X. G. *Organometallics* **2004**, *23*, 3303. (e) Zhou, L. Y.; Yao, Y. M.; Zhang, Y, Sheng, H. T.; Xue, M. Q.; Shen, Q. *Appl. Organomet. Chem.* **2005**, *19*, 398. (f) Zhou, L. Y.; Yao, Y. M.; Zhang, Y.; Xue, M. Q.; Chen, J. L.; Shen, Q. *Eur. J. Inorg. Chem.* **2004**, 2167. (g) Zhang, W. X.; Nishiura, M. Hou, Z. M. *Synlett* **2006**, 1213. (h) Zhang, W. X.; Nishiura, M.; Hou, Z. M. *J. Am. Chem. Soc.* **2005**, *127*, 16788.

(19) (a) Dubé, T.; Freckmann, D.; Conoci, S.; Gambarotta, S.; Yap, G. P. A. *Organometallics* **2000**, *19*, 209. (b) Dubé, T.; Gambarotta, S.; Yap, G. P. A. *Organometallics* **2000**, *19*, 817. (c) Wang, J.; Dick, A. K. J.; Gardiner, M. G.; Yates, B. F.; Peacock, E. J.; Skelton, B. W.; White, A. H. *Eur. J. Inorg. Chem.* **2004**, *10*, 1992.

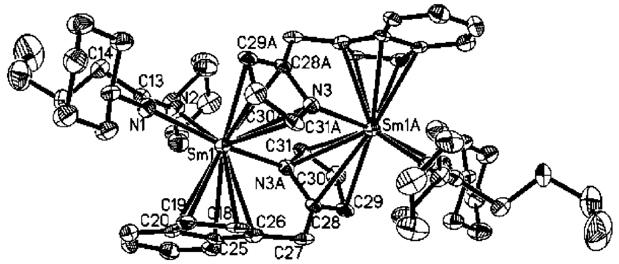

Figure 6. ORTEP diagram of **6** with the probability ellipsoids drawn at the 30% level. Hydrogen atoms are omitted for clarity.

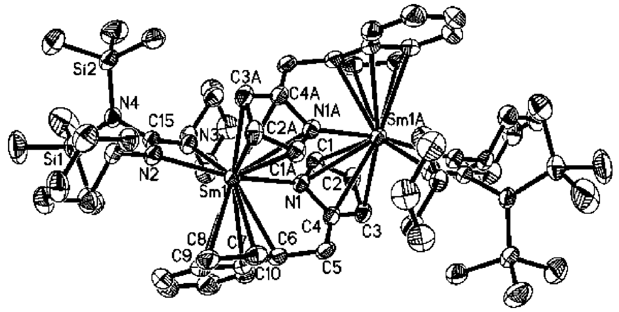

Figure 7. ORTEP diagram of **7** with the probability ellipsoids drawn at the 30% level. Hydrogen atoms are omitted for clarity.

Both **6** and **7** were confirmed by spectroscopic data, elemental analyses, and single-crystal X-ray analyses, which were in good agreement with the proposed formula. The IR spectra of compounds **6** and **7** show typical characteristic $-\mathrm{N}\overset{...}{-}\mathrm{C}\overset{...}{-}\mathrm{N}-$ absorptions at 1649 and 1629 cm^{-1}, respectively. Complexes **6** and **7** are soluble in polar organic solvents such as THF, ether, and toluene but sparely soluble in *n*-hexane.

An X-ray diffraction study shows that complex **6** is a centrosymmetric dimer (Figure 6). The structural data listed in Table 7 indicate that the geometry of the $[(C_9H_6)CH_2(\alpha\text{-}C_4H_3N)]_2Sm_2$ core in **6** is very close to that in **4** with normal bond parameters. The C13−N1 and C13−N2 distances of the amidinate group are approximately equivalent and significantly shorter than the C−N single bond distances, indicating that the π-electrons of the C=N double bond in the present structure are delocalized over the N−C−N unit. Consistent with this, the Sm−N1 and Sm−N2 distances, 2.391(9) and 2.438(9) Å, are intermediate between the values observed for a Sm−N single bond distance and a Sm−N donor bond distance.[20]

Positive structural verification of **7** was also provided by a single-crystal X-ray analysis (Figure 7). Complex **7** is similar to complex **6**, the main difference being the presence of a $N(SiMe_3)_2$ substituent replacing the butyl. As expected, the newly formed guanidinate ligand is bound to Sm through two nitrogen atoms to yield a planar four-membered ring with a bite angle of 54.4(2)°, which is comparable with those in $[(Me_3Si)_2NC(C_6H_{11})_2]_2SmCH(SiMe_3)_2$ (55.1(1)° and 55.6(1)°).[21] The bond angles around C(15) are consistent with sp^2 hybridization. The coordination number of the central Sm^{3+} is nine. The bond lengths of Sm−N3 and Sm−N2 in the delocalized chelating guanidinate ligand are 2.432(4) and 2.444(4) Å, respectively, consistent with the values found in $[(SiMe_3)_2NC(C_6H_{11})_2]_2SmCH(SiMe_3)_2$ [21] and $Sm[Ph_2N(NCy)_2]_3$.[22] The orientation of the $N(SiMe_3)_2$ groups relative to the NCNSm plane is approximately perpendicular, which is identical to the observations in other guanidinate lanthanide complexes.[23] This disposition prevents *p*-overlapping between these two moieties; however, it increases the steric bulk above and below the planar guanidinate ligand. As a result, the N4−C15 distance of 1.456(7) Å is significantly longer than the values observed in $(C_5H_5)_2Ln[RNC(NH^iPr)N^iPr]$ (R = ^{t}Bu, Ln = Yb, Er, Dy, Y; R = Ph, Ln = Yb) (1.368(8)−1.378(8) Å).[19d]

Conclusions

A new methylene-bridged indenyl−pyrrolyl hybrid ligand was designed and successfully prepared. Several di- and trivalent organolanthanide complexes derived from this ligand were synthesized and fully characterized. Furthermore, the reactions of their trivalent alkyl and amide derivatives with carbodiimide were also studied. These results show that this ligand possesses not only the common features of both moieties but also versatile coordination chemistry. From the data reported in this work, it seems reasonable to conclude that the bonding mode adopted by $(C_9H_6)CH_2(\alpha\text{-}C_4H_3N)$ is likely directed by the nature of the lanthanide metal and the alkali metal. For example, it can coordinate in μ-η^1:η^5:η^5 or μ-η^1:η^3:η^5 fashion depending on the nature of the lanthanide metals. Furthermore, these results suggest that the present ligand in the bonding modes to metals may be more versatile than the corresponding methylene-bridged cyclopentadienyl−pyrrolyl hybrid ligand. For the latter, only the chelating η^1:η^5-bonding mode is observed.

Acknowledgment. We thank the NNSF of China, NSF of Shanghai, the Fund of the New Century Distinguished Scientist of the Education Ministry of China, and the Research Fund for the Doctoral Program of Higher Education of China for financial support.

Supporting Information Available: Tables of atomic coordinates and thermal parameters, all bond distances and angles, and experimental data for all structurally characterized complexes. This material is available free of charge via the Internet at http://pubs.acs.org.

OM060610T

---

(20) Wang, J.; Gardiner M. G. *Chem. Commun*. **2005**, 1589. Evans, W. J.; Forrestal, K. J.; Ziller, J. W. *J. Am. Chem. Soc.* **1998**, *120*, 9273. Obora, Y.; Ohta, T.; Stern, C. L.; Marks, T. J. *J. Am. Chem. Soc*. **1997**, *119*, 3745. Zhou, X. G.; Zhang, L. B.; Zhu, M.; Cai R. F.; Weng, L. H.; Huang, Z. X.; Wu, Q. J. *Organometallics* **2001**, *20*, 5700.

(21) Zhou, Y. L.; Yap, G. P. A.; Richeson, D. S. *Organometallics* **1998**, *17*, 4387.

(22) Zhou, L. Y.; Yao Y. M.; Zhang, Y.; Xue, M. Q.; Chen, J. L.; Shen, Q. *Eur. J. Inorg. Chem.* **2004**, 2167.

(23) (a) Lu, Z. P.; Yap, G. P. A.; Richeson, D. S. *Organometallics* **2001**, *20*, 706. (b) Giesbrecht, G. R.; Whitener, G. D.; Arnold, J. *J. Chem. Soc., Dalton Trans.* **2001**, 923. (c) Luo, Y. J.; Yao, Y. M.; Shen, Q.; Yu, K. B.; Weng, L. H. *Eur. J. Inorg. Chem.* **2003**, 318.